# Architectural differences in photopolymerized PEG-based thiol-acrylate hydrogels enable enhanced mechanical properties and 3D printability



ARREGUIN CAMPOS, Mariana; Dookhith, Aaliyah Z.; EBRAHIMI, Mahsa; Lynd, Nathaniel A.; Sanoja, Gabriel E.; Aldana, Ana A.; Baker, Matthew B. & PITET, Louis

(2024) Architectural differences in photopolymerized PEG-based thiol-acrylate hydrogels enable enhanced mechanical properties and 3D printability. In: EUROPEAN POLYMER JOURNAL, 212 (Art N° 113070).

DOI: 10.1016/j.eurpolymj.2024.113070
Handle: http://hdl.handle.net/1942/43270

# Architectural differences in photopolymerized PEG-based thiol-acrylate hydrogels enable enhanced mechanical properties and 3D printability

Mariana Arreguín-Campos[1], Mahsa Ebrahimi[1], Aaliyah Z. Dookhith[2], Nathaniel A. Lynd[2], Gabriel E. Sanoja[2], Ana A. Aldana[3], Matthew B. Baker[3*], Louis M. Pitet[1*]

[1]*Advanced Functional Polymers (AFP) Laboratory, Institute for Materials Research (imo-imomec), Hasselt University, Martelarenlaan 42, 3500 Hasselt, Belgium.*

[2]*McKetta Department of Chemical Engineering, The University of Texas at Austin, Austin, Texas 78712, United States.*

[3]*Department of Complex Tissue Regeneration, MERLN Institute for Technology Inspired Regenerative Medicine, Maastricht University, Universiteitssingel 6229 ER Maastricht, The Netherlands.*

**ABSTRACT**

Hydrogels have been widely investigated for applications in the human body due to their tunability and biocompatibility. Nevertheless, their application is still limited by their relatively low mechanical strength relative to load-bearing tissue scaffolds like articular cartilage. In this work, we synthesized hydrogels by combining linear poly(ethylene glycol) dimethacrylate (PEGDMA) with a 3-arm-PEG end-functionalized with thiol. We demonstrate that the combination of thiol-ene click chemistry with a multifunctional crosslinker reduces the crosslink and entanglement density in comparison with the otherwise statistically crosslinked/polymerized PEGDMA, whereby the only viable mode of gelation is through radical propagation or termination at the double bond. The corresponding minimization of topological heterogeneities that arises during thiol-ene crosslinking results in hydrogels with compressive strength in the range of tens of MPa. The molar mass of the linear PEGDMA precursor is readily tunable, unlocking access to a wider range of mechanical properties. We employed photo-mediated crosslinking protocol, which is amenable to advanced processing technologies such as light-based 3D printing techniques. Such advanced fabrication processes offer high precision and control during the generation of customizable macroscopic objects. Simple prototypes were generated using digital light processing (DLP) equipment.

We demonstrate that integrating a simple co-macromonomer into a widely employed hydrogel platform can unlock new mechanical regimes and mitigate the inherent brittleness associated with these materials. The simplicity of this approach, coupled with its easy tunability and adaptability to light-based techniques, holds promise for broadening hydrogel applications in tissue engineering. Our findings contribute to advancing materials and methodologies, facilitating enhanced design and fabrication of functional constructs.

## INTRODUCTION

Hydrogels are crosslinked hydrophilic polymers that are swollen with substantial amounts of water. Due to their unique properties such as biocompatibility, tunable response, and high-water composition, hydrogels are routinely used in various fields ranging from actuators in soft robotics[1] to agriculture[2] and personal care products.[3] Despite possessing several outstanding characteristics, their poor mechanical performance is a recurrent challenge.[4-6] This limitation is particularly relevant when the material is required to endure significant mechanical stresses and strains; for instance, when aiming to restore the functionality of load-bearing tissues such as articular cartilage,[7] tendons[8], and ligaments.[9] While hydrogels excel in providing a hydrated and biocompatible environment for cell growth, their inherent softness and brittleness hinders their broader application.

To address this limitation, it is critical to understand the fundamental relationship between network (molecular) topology and constitutive units and how these factors influence the mechanical response to external deformation. Harnessing the specificity and efficiency of certain chemical reactions can provide a convenient route to uncovering such relationships.[10-14] Seminal investigations have been performed in hydrogels, revealing the key role that network inhomogeneities play in influencing physical and mechanical properties.[12, 14-23] This relationship between network homogeneity and mechanical properties has also been highlighted for elastomers.[24-31] Such inhomogeneities (e.g., loops, dangling chain ends, entanglements) can affect the load distribution at the molecular scale and restrict the cooperativity of the network, reducing the overall mechanical performance.[32] In recent years, various approaches have been explored to enhance the

mechanical performance of hydrogels by incorporating energy dissipation mechanisms within their structure[33], notably, slide-ring gels,[34, 35] double-network hydrogels,[36, 37] or nanoparticle reinforced hydrogels.[38, 39] Despite the outstanding mechanical properties that such gels, their processability into customizable macroscopic objects is typically limited by the relative complexity of the molecular makeup and tedious preparation protocols.

An alternative approach entails mitigating stress concentrations and the probability of nucleating a crack by forming hydrogels with a homogeneous (i.e., uniform) network. The conceptual simplicity of this approach offers opportunities for straightforward processing, as well as enhancing the mechanical performance. Sakai et al. reported the synthesis of "tetra-PEG" gels, which consist of two symmetrical tetrahedron-like polyethylene glycol macromonomers.[17] The tetrahedron-like structures contained propylamine and succinimidyl glutarate as terminal end groups, forming amide bonds under biological pH. By combining these well-defined molecules, hydrogels with improved mechanical performance (2.5 MPa of compressive stress) were obtained by reducing the heterogeneities linked to a random crosslinking process,[17] where constitutive units and junction functionality are not uniform. Malkoch M et al. reported the formation of well-defined hydrogels using click chemistry by combining diacetylene-functionalized and tetraazide-functionalized polyethylene glycol (PEG) derivatives.[40] Gels were made in the presence of copper sulfate and sodium ascorbate as a reducing agent. By varying the molecular weight of PEG, the mechanical properties could be tailored, reaching an ultimate tensile strength of 2.4 MPa for hydrogels with a number average molar mass between crosslinks ($M_x$) of 10 kg/mol.

Such relatively simple, one-step synthetic approaches not only enable remarkably strong gels, but they offer opportunities for advanced processing. Particularly, reactions that can be initiated with light are ideally suited for vat photopolymerization-based 3D printing techniques, having drawn significant attention due to advantages of high precision and speed (relative to other 3D printing technologies).[41] With the aim of employing UV-light to process hydrogels into complex structures, we combine linear PEG-dimethacrylate (PEGDMA) with a 3-arm-PEG end-functionalized with thiol. We chose to implement a 3-arm PEG-SH molecule to highlight the contrast between network architectures arising from the use of either

(1) PEG-DMA telechelic molecules alone vs. (2) a well-defined multi-functional crosslinker having a specific reactive handle. We make use of thiol-ene click chemistry for a fast and selective reaction, reducing the degree of freedom that arises from a randomized radical reaction among pure PEGDMA-based networks. Thiol-ene chemistry is widely utilized in the construction of complex macromolecular materials.[42-45] Its popularity is attributed to the ready availability of a diverse array of both thiols and enes, coupled with the ease of synthetic strategies, insensitivity to water and oxygen, and the feasibility of working under mild conditions.[46-49] Roquart et al. describe polymeric systems that combine acrylate-functionalized PEG homopolymerization with thiol-ene reactions, referring to them as thiol-acrylate networks.[42] They demonstrate that achieving a sufficient thiol to acrylate ratio suppresses the homopolymerization of acrylates, resulting in material properties determined by the network topology derived from the thiols used (tetrafunctional and monofunctional). Additionally, they observe that the use of relatively longer PEGDA chains (Mn = 3200 g/mol) further decreases the contribution of acrylate homopolymerization to crosslinking. In this work, we make use of a range of linear PEGDMAs with varying molar mass (starting at 6 000 g/mol) to enable the fine-tuning of the mechanical properties of the gel. The stress-stretch curves are analyzed within the molecular model of Rubinstein-Panyukov on entangled networks to quantify the densities of crosslinks and entanglements and understand their contributions to the mechanical properties. Consequently, we are able to map out a wide spectrum of material formulations that should prove very powerful in expanding the range of applications for which hydrogels are suitable.

## RESULTS AND DISCUSSION

With the goal of achieving hydrogels with a better-defined network architecture and easy customization, we synthesized hydrogels by combining linear PEG with varying molecular weights with a 3-arm PEG as a multifunctional crosslinker. Linear PEG of 6 000, 10 000, and 20 000 g/mol were end-functionalized with methacrylic anhydride using a microwave reactor, resulting in PEGDMA. Next to this, 3-arm PEG of 1 000 g/mol was reacted with 3-mercapto propionic acid under Dean-stark conditions,

yielding 3armPEG-SH. In short, hydrogels were made by combining both macromonomers in water in a constant 1:1 ratio of thiol to methacrylate groups. An unchanging concentration of 0.3 wt% of Lithium phenyl (2,4,6-trimethylbenzoyl) phosphinate (LAP) was used as photo-initiator. The compounds were dissolved in distilled water and mixed until clear solutions were obtained, poured into molds, and then exposed to UV light (254 nm, 40 Watt) in an oven for 15 minutes to undergo crosslinking (See Supporting Information for more details on polymer and hydrogel synthesis). We hypothesized that by adding a multi-arm crosslinker, the network architecture would be more uniform compared to using only PEGDMA, which gels via a free-radical crosslinking route. Specifically, we consider a uniform network to possess a spatially homogeneous distribution of crosslinks and a consistent crosslink junction functionality. A very ideal schematic depiction of the two alternative scenarios is illustrated in Figure 1. A network generated exclusively from PEGDMA will react to give rise to shorter intermediate chains with a statistically distributed degree of polymerization, creating a dense and relatively non-uniform network architecture with a variable number of chains emanating from the various crosslinking junctions (Figure 1A). In contrast, when a 3-arm molecule comprising selective, complementary reactive groups (i.e., thiols) is introduced as a crosslinker, the number of chains converging at each crosslink is restricted to three, resulting in a more consistent junction functionality, thus, a better-defined architecture (Figure 1B). Although two double bonds from PEGDMA can presumably still react with each other in the second scenario, we employed thiol-end-capped units in order to largely prevent the homopolymerization of PEGDMA to favor the thiol-ene click pathway. We hypothesized that such an approach would lead to a more consistent crosslink junction functionality, minimizing the presence of inhomogeneities and leading to a material with improved mechanical performance.

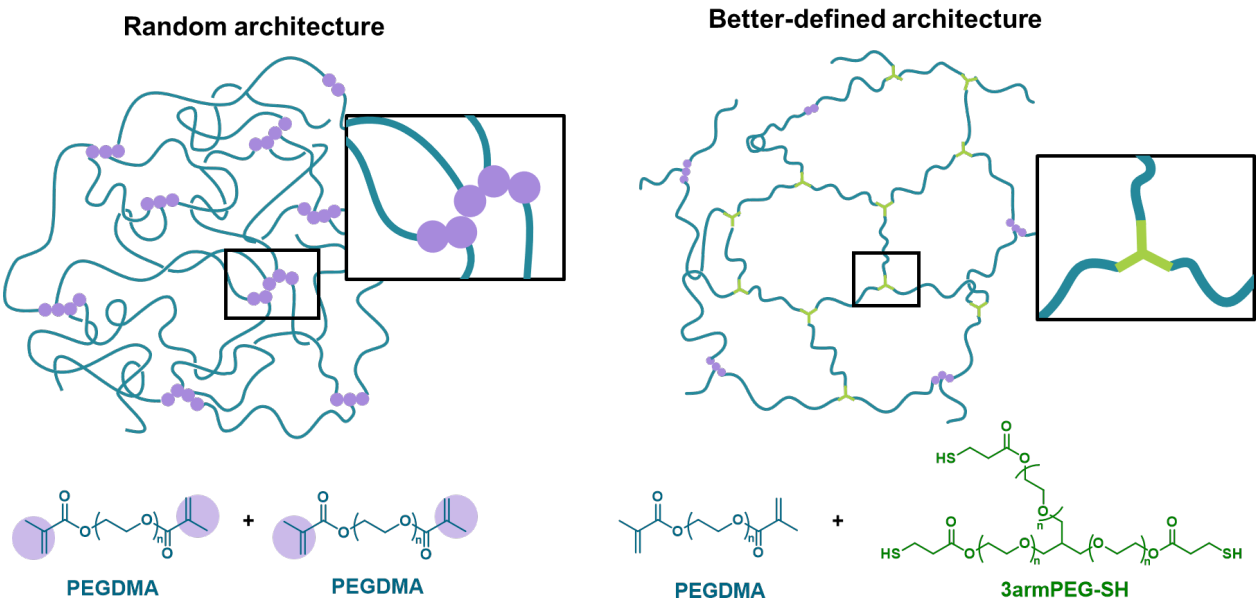


***Figure 1.*** Representation of a randomly crosslinked PEGDMA network vs a well-defined PEGDMA-SH network. The incorporation of a multifunctional crosslinker reduces the number of chains that can come out of each crosslinking point. This provides a more ordered structure compared to the random crosslinking process of PEGDMA where a variable number of chains can come out of each crosslinking point.

The macroscopic influence of the multifunctional crosslinker in generating a material with enhanced mechanical performance is observed through compression and tensile tests. Figure 2A compares two sets of samples that were prepared with identical PEGDMA precursors (molar mass 6 kg/mol) and overall polymer content (20 wt %). The two sample sets differ only in the presence (or absence) of the 3-arm PEG-SH. In samples with PEG-SH, the quantity added was such that the end-group stoichiometry was approximately the same, ranging from 7.8 to 28.3 wt % of the total polymer content, depending on the molar mass of the PEGDMA. The hydrogels containing only PEGDMA fractured before reaching 75% strain under compression while the other set of hydrogels readily reached 90% strain without breaking, which corresponded to a compressive strength of 11 MPa (Figure 2A). The compression modulus is consistent with the PEGDMA-only hydrogels being stiffer, having a value of 830 kPa compared to 480 kPa for those containing thiols. The contrast implies a more densely crosslinked system with PEGDMA alone, highlighting the difference in network connectivity (as shown in Figure 1) reflected by the mechanical performance. Hydrogels made from PEGDMA precursors having molar masses of 10 and 20 kg/mol, and

20 wt% polymer content, were also tested and compared with thiol and without thiol (Figure S1). We observed that increasing molar mass between crosslinks led to a significantly smaller contrast between the two types of hydrogels. That is, the mechanical response exhibited by gels made with thiol and without thiol became more similar with increasing molar mass. This effect can be associated to the total number of (chemical) crosslinks being diluted as the molecular weight increases, concurrent with a variation in entanglement density. As a result, in the case of PEGDMA-SH, mechanical properties are consistent with a looser and softer network possessing fewer entanglements as a result of the more well-defined topology. Conversely, in the PEGDMA-only network, longer strand lengths contribute to enhanced stretchability and reduced brittleness. However, due to the expected higher presence of inhomogeneities, particularly entanglements arising from denser crosslinking points, PEGDMA-only exhibits higher crosslink density demonstrating a higher maximum stress. The contrasting network architectures are corroborated by modeling (*vide infra*). Furthermore, the influence of entanglements on the physical properties becomes increasingly pronounced as the molecular weight surpasses the critical entanglement molecular weight (ca. 2 kg/mol for PEG)[50], and the overlap concentration (ranging between 5 – 12 wt% for PEG 6 , 10 and 20 kDa).[51, 52]

The molecular model of Rubinstein and Panyukov was used to interpret the mechanical response of both families of hydrogels, which strain soften when entangled. The crosslink and entanglement density were quantified by fitting the stress-strain curves in tension (Figure S2) to the following equation:

$$\sigma_N = \left(\nu_x + \frac{\nu_e}{0.74\lambda + 0.61\lambda^{-0.5} - 0.35}\right) k_B T \left(\lambda - \frac{1}{\lambda^2}\right)$$

Where $\lambda$, $\nu_x$, and $\nu_e$ are respectively the stretch, the density of elastic chains and the density of entanglements. We determined the ratio of crosslinks to entanglements for samples prepared with 6,10, and 20 kg/mol of PEGDMA. In the presence of thiol, the ratios were 10.2, 5.6, and 4.1, while in its absence, they were 11.8, 10.1 and 0.9, respectively. Figure 2B graphically illustrates the contrasting contributions

from the entanglement and crosslink density. The data reveals that for hydrogels without thiol, a higher crosslink density develops, which is substantially higher than the sample incorporating the 3-arm-thiol. Moreover, the samples with a molecular weight of 20 kDa and no thiol, highlight the large presence of entanglements when the molecular weight is increased. These results support the proposed hypothesis, demonstrating a clear connection between the reduction of entanglements and crosslink density, attributed to the architectural differences resulting from the incorporation of our multifunctional crosslinker.

This difference in network architecture results in materials exhibiting improved mechanical performance. Specifically, these materials demonstrate increased resilience, allowing them to endure larger strain and higher stress, suggesting a more well-defined network architecture.

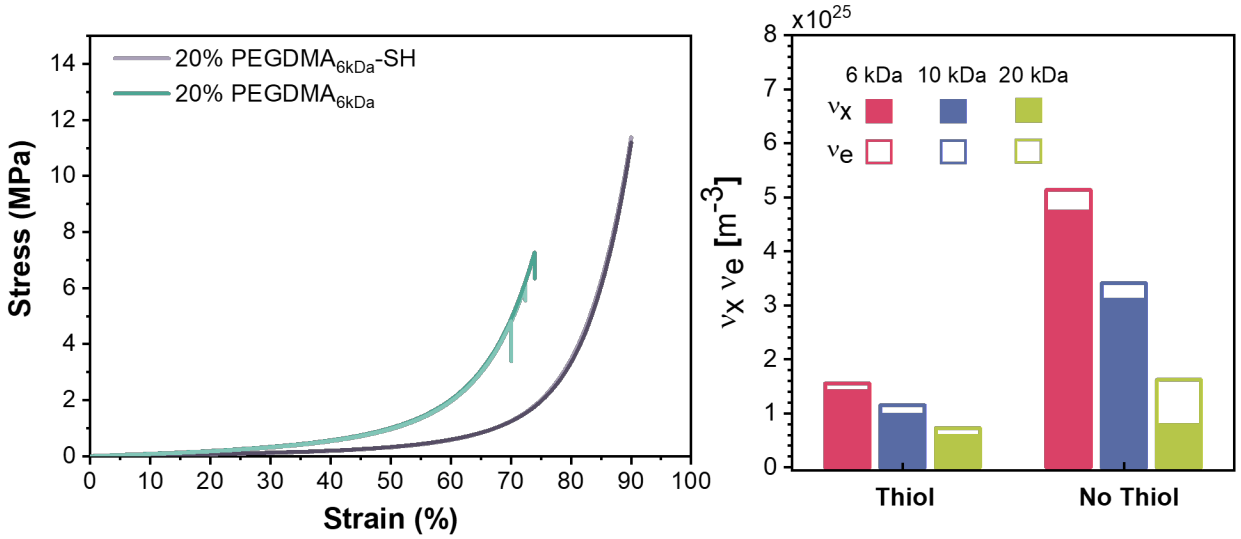


***Figure 2.*** Mechanical comparison of PEGDMA vs PEGDMA-SH network. A. Compression results of samples containing 20 wt % polymer and 6 kDa PEGDMA displaying a larger strain and higher stress when thiol is incorporated. Curves in different shades of the same color correspond to runs obtained from triplicates. B. Entanglement and crosslink density values obtained from fitted tensile data using Rubinstein and Panyukov model. Results demonstrate lower crosslink density and less entanglements when thiol is present.

In order to further unveil the structure-property relationships, we employed three different linear PEGDMA precursors differing in molar mass (6, 10 and 20 kg/mol) and three different polymer concentrations (15, 20, 25 w/w %). The same 3-arm-PEG thiol compound ($M_n$ = 1 kg/mol) was used as the multifunctional linker in all the experiments in a constant 1:1 ratio of thiol to methacrylate groups, representing around 7.8

to 28.3 wt % of the total polymer content, depending on the molar mass of the PEGDMA. Samples were prepared in triplicates and their mechanical performance was recorded under tensile and compression (Figure 3). Generally, increasing the molar mass of the linear PEG results in softer gels that can readily be compressed to 90% strain without breaking. Tensile measurements also reveal relatively high extensibility, reaching around 500 % for the sample made from 10 kg/mol PEG precursor (Figure 3B). The relatively short PEG-units (6 kg/mol) possess a correspondingly low molar mass between crosslinks ($M_x$), resulting in a stiffer, more densely crosslinked network. As a consequence, $PEGDMA_{6k}$ samples consistently fractured at lower strains during elongation, but they could withstand larger compressive stress (11 MPa with 20 wt%). This trend is also supported with the Young's modulus, whereby lower molar mass PEGDMA segments (i.e., lower $M_x$) exhibit higher modulus (Figure 3C, D). These results are consistent with literature, linking decreased density of polymer chains with longer polymer segments between crosslink junctions.[53, 54] Similarly, the stiffness of hydrogels increases monotonically with increasing polymer concentration (or decreasing water content) at a fixed $M_x$. Moreover, the Young's modulus values are notably higher under compression compared to those under tensile, which has also been observed in similar hydrogel systems.[55, 56] The mechanical properties of the hydrogels with the different concentrations and molecular weight variations can be found in the Supporting Information (Figure S3).

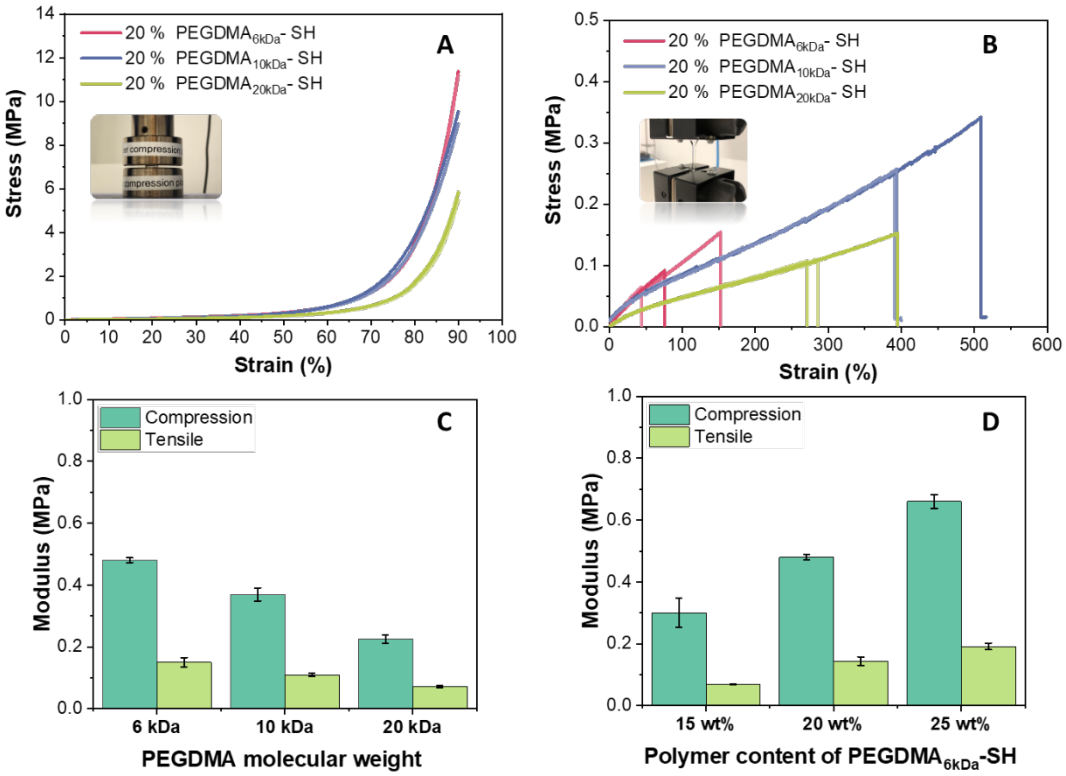


***Figure 3.*** Characterization of single network PEGDMA/3armPEG-SH gels varying molecular weights. Mechanical performance under A. compression and B. tensile of hydrogels with 20 wt % while varying the molecular weight of the PEGDMA segment. Curves in different shades of the same color correspond to runs obtained from their triplicates. **C**. Modulus comparison of gels under compression and tensile. D. Comparison of tensile and compression Young's Modulus obtained for gels made with PEGDMA 6kDA. Error bars correspond to standard deviation obtained from triplicates.

The thiol-ene reaction proceeds via radical addition upon irradiation, and the polymer scaffold is constructed via a step-growth mechanism. However, the methacrylates can also readily homopolymerize via a chain-growth mechanism in the presence of radicals.[57] Thus, when synthesizing hydrogels comprising thiol and vinyl groups via UV-irradiation, the resulting network will be comprised of a mixture of homopolymerized PEGDMA and thiol-ene connected PEGDMA as described by Roquart et al.[42] We compared the reaction kinetics considering the competing pathways by measuring the in-situ crosslinking time via rheological analysis during irradiation (405 nm). Two sets of samples were prepared using the same linear $PEGDMA_{10k}$ precursor and overall polymer content (20 wt %); one sample contained the multi-functional crosslinker and one sample did not. Time sweeps were conducted (Figure 4), during which it was observed that the reactions occurred at a similar rate, suggesting that both reactions (thiol-ene and

PEGDMA homopolymerization) occur at similar rate. However, it is known that in the presence of oxygen, photoinitiator and spreading monomer radicals generate peroxy radicals, thereby inhibiting PEGDMA chain-growth polymerization.[58, 59] Contrary to this, step-growth polymerization of thiol with a vinyl group can be propagated by the formed reactive oxygen species, ultimately favoring the thiol-ene reaction over methacrylate homopolymerization.[47, 60] Furthermore, Figure 5 shows the time sweep data of hydrogels formed using different formulations, highlighting the effect of polymer content and molar mass on the crosslinking time and shear modulus. The experiments were conducted such that irradiation was initiated after running for 2 min in the dark. The time required to reach the plateau in storage modulus (G') decreases with increasing precursor molar mass, for a fixed polymer content. This is in line with the Flory-Stockmayer gel point theory, wherein the proportion of bonds necessary to achieve gelation decreases as the molecular weight increases (Figure 5A).[61] In contrast, the crosslinking time decreases with increasing polymer content/concentration at a fixed precursor molar mass, where the concentration of reactive end-groups increases the overall kinetics when the polymer content increases (Figure 5B). Additionally, the higher dilution may lead to more intramolecular cyclization, delaying the gelation at lower polymer concentration.

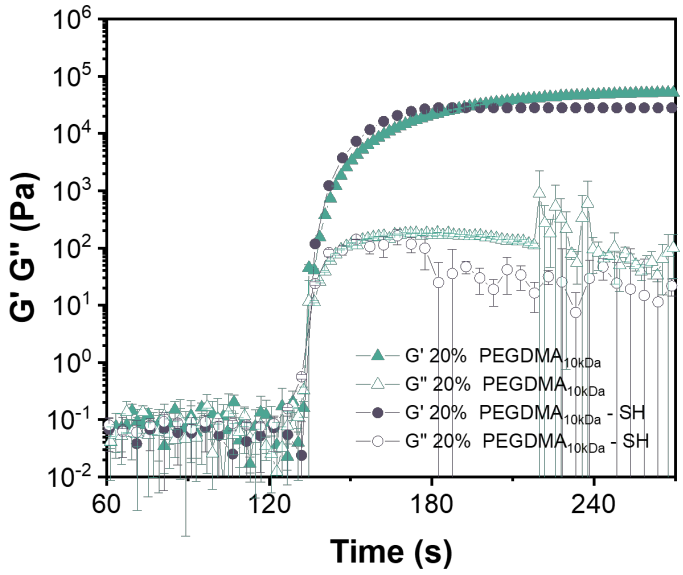


***Figure 4.*** In-situ crosslinking of two sets of samples, one containing thiol and one without. Time-sweep rheological analysis of samples with an overall 20 wt % polymer content and 10 kDa PEGDMA.

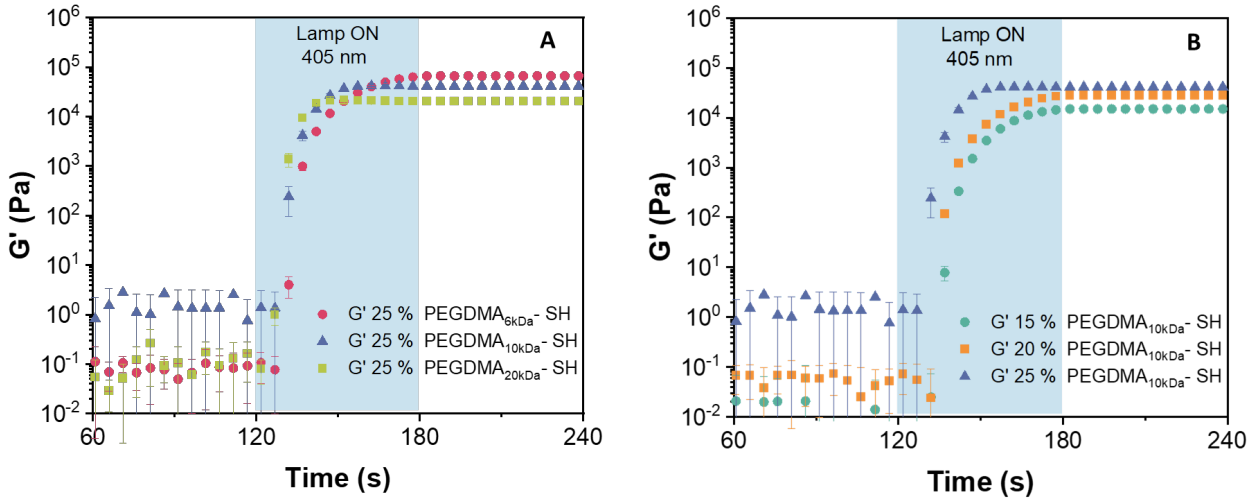


***Figure 5.*** Comparison of the crosslink kinetics of hydrogels varying A. Molecular weight and B. polymer content. Time required to obtain complete crosslink (when the plateau is reached) increases inversely with molecular weight and polymer content.

The swelling of hydrogels was investigated for the series of molar mass linear precursors ranging from 2–20 kg/mol (Table 1). Formulations containing complementary thiol and methacrylate functionalized building blocks were evaluated for all the different molar masses of linear PEGDMA (6, 10 and 20 kg/mol), including an extra formulation using PEGDMA 2 kg/mol. For a comparison of resulting architectures, two samples were prepared without the thiol (i.e., homopolymerization dominated) using the 2 kg/mol and 6 kg/mol precursors. The gel fraction (GF) is consistently high (≥ 94%), with the exception of two samples: 2 kg/mol 20% PEGDMA-SH and 20 kg/mol 20% PEGDMA-SH. These gel fractions suggest some amount of unreacted thiol, which would impact the network topology. Nevertheless, the gel fraction is still rather high (88% for $PEGDMA_{2kDa}$-SH and 90 % for $PEGDMA_{20kDa}$-SH), even for these two samples. We consider that swelling behavior is dominated by the molar mass of the linear components (i.e., $M_x$), since the mass percent of polymer is identical in all samples. As such, the swelling factor increase monotonically with increasing precursor molar mass. Furthermore, the swelling factor is higher in samples containing the thiol. This behavior is consistent with molecular swelling theories,[62] wherein a slightly higher molar mass between crosslinks allows for more water to osmotically swell within the network. The multifunctional thiol allows a more homogeneous distribution of the chain lengths and reduces the occurrence of shorter chains in the architecture as opposed to the networks formed in its absence. This observation is consistent

with the mechanical properties, providing additional support for the proposed better-defined network architecture. Mesh size (**ξ**), as calculated by the Flory-Rehner equation (see Supporting Information), is similarly related to the segment lengths between two adjacent crosslinks. As such, ξ increases proportionally with molar mass and is larger for samples in which the multifunctional thiol is present. This additional factor is further consistent with the argument related to architecture and network uniformity. Likewise, crosslink density ($\rho_c$) scales along the same trends, consistent with a higher crosslink density arising from the absence of thiol, where the reactions leading to crosslinking are dominated by radical homopolymerization and consequently generating random and denser networks. On top of the statistical nature of the radical chain-polymerization process dominating the PEGDMA crosslinking, chain transfer reactions will contribute further to higher crosslinking densities and hence lower swelling ratios.

**Table 1.** Swelling factor (SF), equilibrium water content (EWC), gel fraction (GF), mesh size, and crosslink density of hydrogels with the same polymer content but variable molecular weight.

| Sample | SF (%)[a] | EWC (%)[b] | GF (%)[c] | ξ (nm)[d] | $\rho_c$ (mol m$^{-3}$)[e] |
|---|---|---|---|---|---|
| 2 kDa 20% PEGDMA | 101 ± 1 | 80 ± 0.1 | 97 ± 2 | 3.0 ± 0.1 | 1500 ± 2 |
| 2 kDa 20% PEGDMA-SH | 133 ± 1 | 86 ± 0.2 | 88 ± 2 | 3.6 ± 0.1 | 1350 ± 12 |
| 6 kDa 18% PEGDMA | 142 ± 1 | 87.2 ± 0.3 | 98 ± 2 | 5.3 ± 0.1 | 626 ± 14 |
| 6 kDa 20% PEGDMA-SH | 261 ± 5 | 92.4 ± 0.1 | 94 ± 1 | 7.5 ± 0.1 | 409 ± 2 |
| 10 kDa 20% PEGDMA-SH | 275 ± 4 | 92.2 ± 0.1 | 98 ± 1 | 9.1 ± 0.1 | 296 ± 2 |
| 20 kDa 20% PEGDMA-SH | 496 ± 10 | 96.3 ± 0.1 | 90.3 ± 0.2 | 17.1 ± 0.1 | 129.2± 0.1 |

[a]**SF** determined as percentage by dividing the mass at equilibrium by the initial after-curing mass. [b]**EWC** is calculated by dividing the difference of the swollen minus the dry weight over the swollen weight. [c]**GF** refers to the initial dry weight over the dry weight after removing unreacted material. [d]**ξ** and [e]**$\rho_c$** are calculated using the Flory-Rehner equation.

The ability to fabricate customized, intricate three-dimensional structures from hydrogel materials holds significant importance in the field of biomaterials from drug delivery to personalized tissue engineering implants.[63, 64] Furthermore, developing high-strength scaffolds via traditional fabrication techniques poses an additional challenge.[65, 66] Among the available fabrication techniques used in bioengineering, photopolymerization-based methods have drawn major attention for generating complex structures due to the advantages of high precision and speed.[41, 67] Digital light processing is a vat-photopolymerization

additive manufacturing technique that enables the fabrication of 3D constructs with high resolution in a layer-by-layer fashion. We were keen to exploit the fast gelation and photo-mediated nature of the thiol-ene crosslinking in our system to generate well-defined custom-made objects using DLP. Samples with complementary thiol-methacrylate building blocks were routinely shown to gel within seconds upon light exposure (405 nm; see Figure 5), making them ideal candidates for DLP fabrication. We explored the PEGDMA-SH hydrogel series for DLP fabrication using a custom-built printer (see Supporting Information; Figure S4). We first optimized the time required for printing a single simple geometry (i.e., 2D experiments). Polymer resin (25 wt % $PEGDMA_{10k}$-SH) was poured over a glass slide and placed above the light source of the DLP. Figure 6A shows the glass slide after being exposed to light. A pattern of a solid square within a hollow concentric square was projected in 8 different positions along the slide while varying the irradiation time in each position (Figure 6B). We observed that a minimum of 12 seconds was required to form a well-defined layer visible to the naked eye. Nevertheless, at 8 seconds, we observed a thin layer of gelation, which could be used for high-resolution constructs. Figure 6C shows that the obtained structures are robust enough to be taken from the glass slide and show good feature reconstruction. Following this, we proceeded to print a cylinder of 8.6 mm (as illustrated in Figures 6D and E) and a ring of 10 mm diameter having 3 mm wall thickness (Figure 6F), to assess the ability to print multi-layered structures. A video showcasing the 3D printing process can be found under the Supplementary Information. To ensure the fabrication of precise shapes, it was found necessary to incorporate tartrazine as a photo absorber at a concentration of 0.11 mg/mL, along with the utilization of an absorptive neutral density filter with an optical density of 0.6. Even though these experiments represent a step towards processing 3D constructs, exploring other parameters is required before other more complex structures can be obtained and will be pursued in our follow-up studies. Nonetheless, these results highlight the potential of our material for digital light processing, offering the prospect of materials endowed with both requisite strength and tailored structures.

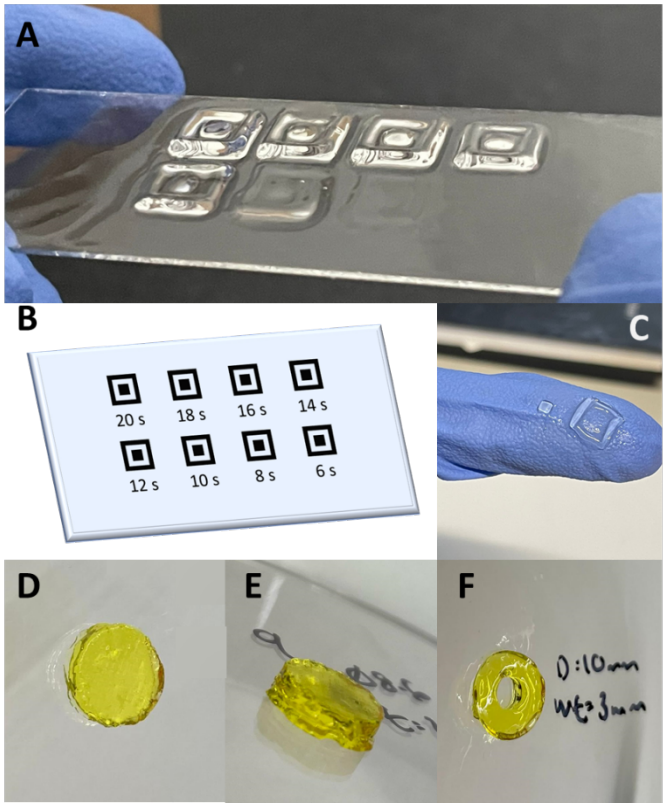


***Figure 6.*** Digital light processing of PEGDMA$_{10kDa}$-SH (25 wt%). A. Image of the crosslinked printed samples on a glass plate with different exposure times, as illustrated schematically in B. C. The individual hydrogel objects as printed, removed and placed on a fingertip to demonstrate mechanical integrity and resolution. D-F. Cylinder and ring featuring layers of 0.1 mm thickness with an exposure time of 5 seconds per layer, resulting in a final height of 3 mm.

## CONCLUSIONS

Understanding the fundamental relationships between network architecture and the constitutive polymers is highly relevant for developing hydrogels with improved mechanical performance. Gels prepared using macromonomers of well-defined molecular weights, and crosslinked through the use of site-specific chemical reactions, prove to possess lower entanglement and crosslink density than analogues prepared from a random crosslinking process. These more homogeneous gels exhibit enhanced mechanical performance and are less prone to early rupture.

In this work, PEG-based hydrogels were synthesized using both a conventional methacrylate radical polymerization and a more selective thiol-ene photopolymerization reaction. The incorporation of a multifunctional thiol crosslinker combined with thiol-ene click chemistry results in an increased elongation and maximum stress (Compressive strength ~ tens of megapascals). Although the use of asymmetric macromonomers does not result in a perfectly homogeneous network, the rapid nature of thiol-ene click chemistry facilitates the enhancement of the performance of hydrogels. This enables straightforward tunability through the linear PEGDMA segment and offers opportunities for advanced processing. Depending on the hydrogel concentration and molecular weight, the crosslinking time ranges from 15 seconds to 1 minute. By making use of linear PEGDMA, the length of the hydrophilic segment can be varied, unlocking a wider range of mechanical properties that could target different applications with the same system. Through swelling, mechanical characterization, and molecular modeling we found that gels made of only PEGDMA possessed a higher crosslink density and entanglement density compared to those with same composition and thiol. PEGDMA-SH hydrogels were proven to have enhanced mechanical properties compared to that of homopolymerized PEGDMA, linked to a better-defined network architecture. Lastly, we showcased the amenability of this system to create simple structures through digital light processing, highlighting our material's potential for producing customized architectures. Our work shows that modifications to existing and widely used hydrogel platforms can unlock new mechanical regimes and alleviate common pitfalls like brittleness. By employing a co-macromonomer that enables better defined crosslinking chemistry, this simple strategy contributes to advancing the design of biomedical hydrogels and enable more effective biofabrication approaches.

## ASSOCIATED CONTENT

### Supporting Information

## AUTHOR INFORMATION

### Corresponding author

*E-mail: louis.pitet@uhasselt.be; Tel. +32 11 26 83 20

*E-mail: matthew.baker@maastrichtuniversity.nl

**Notes**

**ORCID**

Louis M. Pitet: https://orcid.org/0000-0002-4733-0707

Mariana Arreguín-Campos: https://orcid.org/0000-0002-7679-6100

Aaliyah Z. Dookhith: https://orcid.org/0000-0003-4219-5515

Gabriel E. Sanoja: https://orcid.org/0000-0001-5477-2346

**ACKNOWLEDGMENTS**

The authors gratefully acknowledge funding for this work from the Research Foundation Flanders (FWO) under contract G080020N. This project has received funding from the European Union's Horizon 2020 research and innovation program under the Marie Skłodowska-Curie grant agreement No 101028471. Additionally, partial support from the Dutch Ministry of Economic Affairs is acknowledged.

**REFERENCES**

(1) Banerjee, H.; Suhail, M.; Ren, H. Hydrogel actuators and sensors for biomedical soft robots: brief overview with impending challenges. *Biomimetics* **2018**, *3* (3), 15.
(2) Kaur, P.; Agrawal, R.; Pfeffer, F. M.; Williams, R.; Bohidar, H. B. Hydrogels in Agriculture: Prospects and Challenges. *Journal of Polymers and the Environment* **2023**, 1-18.
(3) Majcher, M. J.; Hoare, T. *14. Applications of hydrogels*; Springer Nature Switzerland AG, 2019.
(4) Sun, J.-Y.; Zhao, X.; Illeperuma, W. R.; Chaudhuri, O.; Oh, K. H.; Mooney, D. J.; Vlassak, J. J.; Suo, Z. Highly stretchable and tough hydrogels. *Nature* **2012**, *489* (7414), 133-136.
(5) Calvert, P. Hydrogels for soft machines. *Advanced materials* **2009**, *21* (7), 743-756.
(6) Zhang, L.; Ma, W.; Tang, H.; Yu, Y.; Wang, L.; Li, T.; Fang, Z.; Qiao, Z. Tough, low-friction and homogeneous physical hydrogel by a solvent-inducted strategy. *Chemical Engineering Journal* **2023**, *466*, 143195.
(7) Adams, M.; Kerin, A.; Wisnom, M. Sustained loading increases the compressive strength of articular cartilage. *Connective tissue research* **1998**, *39* (4), 245-256.
(8) Shadwick, R. E. Elastic energy storage in tendons: mechanical differences related to function and age. *Journal of applied physiology* **1990**, *68* (3), 1033-1040.
(9) Zhao, X.; Chen, X.; Yuk, H.; Lin, S.; Liu, X.; Parada, G. Soft materials by design: unconventional polymer networks give extreme properties. *Chemical Reviews* **2021**, *121* (8), 4309-4372.

(10) Li, Y.; Wang, X.; Han, Y.; Sun, H.-Y.; Hilborn, J.; Shi, L. Click chemistry-based biopolymeric hydrogels for regenerative medicine. *Biomedical Materials* **2021**, *16* (2), 022003.
(11) Zou, Y.; Zhang, L.; Yang, L.; Zhu, F.; Ding, M.; Lin, F.; Wang, Z.; Li, Y. "Click" chemistry in polymeric scaffolds: Bioactive materials for tissue engineering. *Journal of controlled release* **2018**, *273*, 160-179.
(12) Barney, C. W.; Ye, Z.; Sacligil, I.; McLeod, K. R.; Zhang, H.; Tew, G. N.; Riggleman, R. A.; Crosby, A. J. Fracture of model end-linked networks. *Proceedings of the National Academy of Sciences* **2022**, *119* (7), e2112389119.
(13) Arora, A.; Lin, T.-S.; Beech, H. K.; Mochigase, H.; Wang, R.; Olsen, B. D. Fracture of polymer networks containing topological defects. *Macromolecules* **2020**, *53* (17), 7346-7355.
(14) Zhong, M.; Wang, R.; Kawamoto, K.; Olsen, B. D.; Johnson, J. A. Quantifying the impact of molecular defects on polymer network elasticity. *Science* **2016**, *353* (6305), 1264-1268.
(15) Shibayama, M. Universality and specificity of polymer gels viewed by scattering methods. *Bulletin of the Chemical Society of Japan* **2006**, *79* (12), 1799-1819.
(16) Li, C.; Wang, Z.; Wang, Y.; He, Q.; Long, R.; Cai, S. Effects of network structures on the fracture of hydrogel. *Extreme Mechanics Letters* **2021**, *49*, 101495.
(17) Sakai, T.; Matsunaga, T.; Yamamoto, Y.; Ito, C.; Yoshida, R.; Suzuki, S.; Sasaki, N.; Shibayama, M.; Chung, U.-i. Design and fabrication of a high-strength hydrogel with ideally homogeneous network structure from tetrahedron-like macromonomers. *Macromolecules* **2008**, *41* (14), 5379-5384.
(18) Kim, J.; Zhang, G.; Shi, M.; Suo, Z. Fracture, fatigue, and friction of polymers in which entanglements greatly outnumber cross-links. *Science* **2021**, *374* (6564), 212-216.
(19) Zhou, H.; Woo, J.; Cok, A. M.; Wang, M.; Olsen, B. D.; Johnson, J. A. Counting primary loops in polymer gels. *Proceedings of the National Academy of Sciences* **2012**, *109* (47), 19119-19124.
(20) Lindemann, B.; Schröder, U. P.; Oppermann, W. Influence of the cross-linker reactivity on the formation of inhomogeneities in hydrogels. *Macromolecules* **1997**, *30* (14), 4073-4077.
(21) Kizilay, M. Y.; Okay, O. Effect of hydrolysis on spatial inhomogeneity in poly (acrylamide) gels of various crosslink densities. *Polymer* **2003**, *44* (18), 5239-5250.
(22) Kuru, E. A.; Orakdogen, N.; Okay, O. Preparation of homogeneous polyacrylamide hydrogels by free-radical crosslinking copolymerization. *European polymer journal* **2007**, *43* (7), 2913-2921.
(23) Di Lorenzo, F.; Seiffert, S. Nanostructural heterogeneity in polymer networks and gels. *Polymer Chemistry* **2015**, *6* (31), 5515-5528.
(24) Luo, J.; Zhao, X.; Ju, H.; Chen, X.; Zhao, S.; Demchuk, Z.; Li, B.; Bocharova, V.; Carrillo, J.-M. Y.; Keum, J. K.; et al. Highly Recyclable and Tough Elastic Vitrimers from a Defined Polydimethylsiloxane Network. *Angew. Chem. Int. Ed.* **2023**, *62* (47), e202310989. DOI: https://doi.org/10.1002/anie.202310989.
(25) Patel, S. K.; Malone, S.; Cohen, C.; Gillmor, J. R.; Colby, R. H. Elastic modulus and equilibrium swelling of poly (dimethylsiloxane) networks. *Macromolecules* **1992**, *25* (20), 5241-5251.
(26) Genesky, G. D.; Cohen, C. Toughness and fracture energy of PDMS bimodal and trimodal networks with widely separated precursor molar masses. *Polymer* **2010**, *51* (18), 4152-4159.
(27) Yoo, S. H.; Yee, L.; Cohen, C. Effect of network structure on the stress–strain behaviour of endlinked PDMS elastomers. *Polymer* **2010**, *51* (7), 1608-1613.

(28) Cristiano, A.; Marcellan, A.; Long, R.; Hui, C. Y.; Stolk, J.; Creton, C. An experimental investigation of fracture by cavitation of model elastomeric networks. *Journal of Polymer Science Part B: Polymer Physics* **2010**, *48* (13), 1409-1422.
(29) Dookhith, A. Z.; Lynd, N. A.; Creton, C.; Sanoja, G. E. Controlling Architecture and Mechanical Properties of Polyether Networks with Organoaluminum Catalysts. *Macromolecules* **2022**, *55* (13), 5601-5609.
(30) Dookhith, A. Z.; Lynd, N. A.; Sanoja, G. E. Tailoring Rate and Temperature-Dependent Fracture of Polyether Networks with Organoaluminum Catalysts. *Macromolecules* **2022**, *56* (1), 40-48.
(31) Mark, J. Polymer Networks. Structure and mechanical properties, AJ Chompff and S. Newman, Eds., Plenum Press, New York, 1971. xiv+ 493 pp. $27.50. *Journal of Polymer Science: Polymer Letters Edition* **1972**, *10* (3), 226-227.
(32) Creton, C. 50th anniversary perspective: Networks and gels: Soft but dynamic and tough. *Macromolecules* **2017**, *50* (21), 8297-8316.
(33) Imran, A. B.; Seki, T.; Takeoka, Y. Recent advances in hydrogels in terms of fast stimuli responsiveness and superior mechanical performance. *Polymer journal* **2010**, *42* (11), 839-851.
(34) Okumura, Y.; Ito, K. The polyrotaxane gel: A topological gel by figure-of-eight cross-links. *Advanced materials* **2001**, *13* (7), 485-487.
(35) Mayumi, K.; Ito, K. Structure and dynamics of polyrotaxane and slide-ring materials. *Polymer* **2010**, *51* (4), 959-967.
(36) Gong, J. P.; Katsuyama, Y.; Kurokawa, T.; Osada, Y. Double-network hydrogels with extremely high mechanical strength. *Advanced materials* **2003**, *15* (14), 1155-1158.
(37) Chen, Q.; Chen, H.; Zhu, L.; Zheng, J. Engineering of tough double network hydrogels. *Macromolecular Chemistry and Physics* **2016**, *217* (9), 1022-1036.
(38) Hu, X.; Liang, R.; Li, J.; Liu, Z.; Sun, G. Mechanically strong hydrogels achieved by designing homogeneous network structure. *Materials & Design* **2019**, *163*, 107547.
(39) Rose, S.; Dizeux, A.; Narita, T.; Hourdet, D.; Marcellan, A. Time dependence of dissipative and recovery processes in nanohybrid hydrogels. *Macromolecules* **2013**, *46* (10), 4095-4104.
(40) Malkoch, M.; Vestberg, R.; Gupta, N.; Mespouille, L.; Dubois, P.; Mason, A. F.; Hedrick, J. L.; Liao, Q.; Frank, C. W.; Kingsbury, K. Synthesis of well-defined hydrogel networks using Click chemistry. *Chemical Communications* **2006**, (26), 2774-2776.
(41) Mo, X.; Ouyang, L.; Xiong, Z.; Zhang, T. Advances in digital light processing of hydrogels. *Biomedical Materials* **2022**, *17* (4), 042002.
(42) Roquart, M.; Kharlamova, A.; Marcos Celada, L.; Norvez, S.; Nicolaÿ, R.; Corté, L. PEG-Based Photo-Cross-Linked Networks with Adjustable Topologies and Mechanical Properties. *Biomacromolecules* **2023**, *24* (10), 4454-4464.
(43) Kalaoglu-Altan, O. I.; Verbraeken, B.; Lava, K.; Gevrek, T. N.; Sanyal, R.; Dargaville, T.; De Clerck, K.; Hoogenboom, R.; Sanyal, A. Multireactive poly (2-oxazoline) nanofibers through electrospinning with crosslinking on the fly. *ACS Macro Letters* **2016**, *5* (6), 676-681.
(44) Khire, V. S.; Harant, A. W.; Watkins, A. W.; Anseth, K. S.; Bowman, C. N. Ultrathin patterned polymer films on surfaces using thiol− ene polymerizations. *Macromolecules* **2006**, *39* (15), 5081-5086.
(45) Cramer, N. B.; Bowman, C. N. Thiol–ene chemistry. *Chemoselective and bioorthogonal ligation reactions: concepts and applications* **2017**, *1*, 117-145.
(46) Kade, M. J.; Burke, D. J.; Hawker, C. J. The power of thiol-ene chemistry. *Journal of Polymer Science Part A: Polymer Chemistry* **2010**, *48* (4), 743-750.

(47) Hoyle, C. E.; Bowman, C. N. Thiol–ene click chemistry. *Angewandte Chemie International Edition* **2010**, *49* (9), 1540-1573.
(48) Sticker, D.; Geczy, R.; Hafeli, U. O.; Kutter, J. P. Thiol–ene based polymers as versatile materials for microfluidic devices for life sciences applications. *ACS applied materials & interfaces* **2020**, *12* (9), 10080-10095.
(49) Resetco, C.; Hendriks, B.; Badi, N.; Du Prez, F. Thiol–ene chemistry for polymer coatings and surface modification–building in sustainability and performance. *Materials Horizons* **2017**, *4* (6), 1041-1053.
(50) Hidema, R.; Fujito, K.-y.; Suzuki, H. Drag force of polyethyleneglycol in flows of polymer solutions measured using a scanning probe microscope. *Soft Matter* **2022**, *18* (2), 455-464.
(51) Zhang, H.; Wehrman, M. D.; Schultz, K. M. Structural changes in polymeric gel scaffolds around the overlap concentration. *Frontiers in chemistry* **2019**, *7*, 317.
(52) Ziębacz, N.; Wieczorek, S. A.; Kalwarczyk, T.; Fiałkowski, M.; Hołyst, R. Crossover regime for the diffusion of nanoparticles in polyethylene glycol solutions: influence of the depletion layer. *Soft Matter* **2011**, *7* (16), 7181-7186.
(53) Macdougall, L. J.; Truong, V. X.; Dove, A. P. Efficient in situ nucleophilic thiol-yne click chemistry for the synthesis of strong hydrogel materials with tunable properties. *ACS Macro Letters* **2017**, *6* (2), 93-97.
(54) Zander, Z. K.; Hua, G.; Wiener, C. G.; Vogt, B. D.; Becker, M. L. Control of Mesh Size and Modulus by Kinetically Dependent Cross-Linking in Hydrogels. *Advanced Materials* **2015**, *27* (40), 6283-6288.
(55) Burke, G.; Cao, Z.; Devine, D. M.; Major, I. Preparation of biodegradable polyethylene glycol dimethacrylate hydrogels via thiol-ene chemistry. *Polymers* **2019**, *11* (8), 1339.
(56) Browning, M.; Wilems, T.; Hahn, M.; Cosgriff-Hernandez, E. Compositional control of poly (ethylene glycol) hydrogel modulus independent of mesh size. *Journal of Biomedical Materials Research Part A* **2011**, *98* (2), 268-273.
(57) Cramer, N. B.; Bowman, C. N. Kinetics of thiol–ene and thiol–acrylate photopolymerizations with real-time fourier transform infrared. *Journal of Polymer Science Part A: Polymer Chemistry* **2001**, *39* (19), 3311-3319.
(58) Mandal, J.; Zhang, K.; Spencer, N. D. Oxygen inhibition of free-radical polymerization is the dominant mechanism behind the "mold effect" on hydrogels. *Soft Matter* **2021**, *17* (26), 6394-6403.
(59) Debroy, D.; Oakey, J.; Li, D. Interfacially-mediated oxygen inhibition for precise and continuous poly (ethylene glycol) diacrylate (PEGDA) particle fabrication. *Journal of colloid and interface science* **2018**, *510*, 334-344.
(60) Nagarjuna, R.; Saifullah, M. S.; Ganesan, R. Oxygen insensitive thiol–ene photo-click chemistry for direct imprint lithography of oxides. *RSC advances* **2018**, *8* (21), 11403-11411.
(61) Stauffer, D.; Coniglio, A.; Adam, M. Gelation and critical phenomena. In *Polymer networks*, Springer, 2005; pp 103-158.
(62) Flory, P. J.; Rehner Jr, J. Statistical mechanics of cross-linked polymer networks II. Swelling. *The journal of chemical physics* **1943**, *11* (11), 521-526.
(63) Li, J.; Wu, C.; Chu, P. K.; Gelinsky, M. 3D printing of hydrogels: Rational design strategies and emerging biomedical applications. *Materials Science and Engineering: R: Reports* **2020**, *140*, 100543.
(64) Chen, Z.; Zhao, D.; Liu, B.; Nian, G.; Li, X.; Yin, J.; Qu, S.; Yang, W. 3D printing of multifunctional hydrogels. *Advanced Functional Materials* **2019**, *29* (20), 1900971.

(65) Xu, C.; Dai, G.; Hong, Y. Recent advances in high-strength and elastic hydrogels for 3D printing in biomedical applications. *Acta biomaterialia* **2019**, *95*, 50-59.
(66) Zhang, X. N.; Zheng, Q.; Wu, Z. L. Recent advances in 3D printing of tough hydrogels: A review. *Composites Part B: Engineering* **2022**, *238*, 109895.
(67) Ding, H.; Dong, M.; Zheng, Q.; Wu, Z. L. Digital light processing 3D printing of hydrogels: a minireview. *Molecular Systems Design & Engineering* **2022**, *7* (9), 1017-1029.